Protein Science (1994), *3*:2175-2184. Cambridge University Press. Printed in the USA.

Thermodynamic characterization of an equilibrium folding intermediate of staphylococcal nuclease

DONG XIE,[1] ROBERT FOX,[2] AND ERNESTO FREIRE[1]

[1] Department of Biology and the Biocalorimetry Center, The Johns Hopkins University, Baltimore, Maryland 21218
[2] Department of Molecular Biophysics and Biochemistry and the Howard Hughes Medical Institute, Yale University, New Haven, Connecticut 06511

(RECEIVED June 28, 1994; ACCEPTED September 26, 1994)

Abstract

High-sensitivity differential scanning calorimetry and CD spectroscopy have been used to probe the structural stability and measure the folding/unfolding thermodynamics of a $Pro^{117} \rightarrow Gly$ variant of staphylococcal nuclease. It is shown that at neutral pH the thermal denaturation of this protein is well accounted for by a 2-state mechanism and that the thermally denatured state is a fully hydrated unfolded polypeptide. At pH 3.5, thermal denaturation results in a compact denatured state in which most, if not all, of the helical structure is missing and the β subdomain apparently remains largely intact. At pH 3.0, no thermal transition is observed and the molecule exists in the compact denatured state within the 0-100 °C temperature interval. At high salt concentration and pH 3.5, the thermal unfolding transition exhibits 2 cooperative peaks in the heat capacity function, the first one corresponding to the transition from the native to the intermediate state and the second one to the transition from the intermediate to the unfolded state. As is the case with other proteins, the enthalpy of the intermediate is higher than that of the unfolded state at low temperatures, indicating that, under those conditions, its stabilization must be of an entropic origin. The folding intermediate has been modeled by structural thermodynamic calculations. Structure-based thermodynamic calculations also predict that the most probable intermediate is one in which the β subdomain is essentially intact and the rest of the molecule unfolded, in agreement with the experimental data. The structural features of the equilibrium intermediate are similar to those of a kinetic intermediate previously characterized by hydrogen exchange and NMR spectroscopy.

Keywords: differential scanning calorimetry; protein folding intermediates; structural thermodynamics

The protein folding problem is one of the most fundamental problems in biology. A structural and thermodynamic characterization of the intermediate states existing along the folding pathway of a protein will provide important clues regarding the mechanism by which a protein attains its native conformation. Recently, significant developments have been made in the study of protein folding intermediates. Hydrogen exchange experiments and 2-dimensional NMR have been used to provide structural information on both kinetic and equilibrium folding intermediates in several proteins (Hughson et al., 1990; Jeng et al., 1990). On the other hand, the energetics of an increasing number of equilibrium folding intermediates have been measured directly (Kuroda et al., 1992; Griko et al., 1994; K.P. Murphy, A.D. Robertson, N.D. Meadow, S. Roseman, & E. Freire, in prep.). The study of equilibrium intermediates has acquired prominence because an increasing body of evidence suggests that kinetic and equilibrium intermediates share common structural characteristics. For example, it has been shown that the kinetic intermediate existing during the folding of apomyoglobin is structurally similar to the equilibrium intermediate that becomes populated at low pH values (Hughson et al., 1990; Jennings & Wright, 1993). This situation appears to be the same for α-lactalbumin (Ikeguchi et al., 1986). During the last few years, it has become evident that, under certain solvent conditions, some proteins exhibit a significant population of equilibrium folding intermediates (Kuwajima, 1989; Jeng et al., 1990; Goto & Nishikiori, 1991; Jeng & Englander, 1991; Xie et al., 1991). The experimental access to folding intermediates that become populated under equilibrium conditions offers the opportunity for detailed structural studies and accurate measurements of their energetics.

Staphylococcal nuclease and its different variants have been extensively used as a model system to study protein folding. This protein of 149 amino acids (M_r = 16,800 kDa) is composed of a β-sheet subdomain (residues 1-31 and 71-98) formed by two 3-stranded sheets and an α-helical subdomain (residues 32-70 and 99-141) composed of 3 α-helices. Recently, Carra et al.

Reprint requests to: Ernesto Freire, Department of Biology, The Johns Hopkins University, 34th and Charles Streets, Baltimore, Maryland 21218; e-mail: bcc@biocal2.bio.jhu.edu.

(1994a, 1994b) have characterized the energetics of a low pH intermediate under different ionic strength conditions. It was found that under high salt and low pH conditions the protein undergoes 2 distinct transitions and that the α-helical domain becomes disrupted in the first transition.

In this paper we studied the staphylococcal nuclease $Pro^{117} \rightarrow$ Gly variant (P117G) whose structure is known at high resolution (Hynes et al., 1994). It has been shown previously that this mutant is slightly more stable than the wild type and that its unfolding obeys a simpler kinetics due to the removal of the proline residue (Evans et al., 1987; Kuwajima et al., 1991; Nakano et al., 1993). Recently, pulsed hydrogen exchange experiments have revealed the protection pattern of an early folding intermediate of P117G (Jacobs & Fox, 1994). The significant structural features of this intermediate are that the two 3-stranded β-sheets are already formed, whereas the α-helices are not yet stabilized. The result is also consistent with the NMR study of a 136-residue nonsense fragment of staphylococcal nuclease in which a compact denatured state is most populated in the absence of ligand (Shortle & Abergunawardana, 1993).

In this paper we demonstrate that, upon lowering the pH, P117G undergoes partial thermal denaturation to an equilibrium partly folded state. In order to characterize the structure and energetics of this equilibrium folding intermediate, we have performed high-sensitivity differential scanning calorimetry and CD experiments. These experiments indicate that, under conditions in which thermal unfolding proceeds in 2 stages, the β-sheet subdomain is the most stable one. To complement these experiments, we have used a previously developed search algorithm aimed at predicting the structural determinants of folding intermediates (Freire & Xie, 1994; Xie & Freire, 1994a, 1994b). These studies support the notion that the equilibrium folded intermediate stabilized at low pH is structurally similar to the kinetic intermediate identified by pulsed hydrogen exchange.

Results and discussion

Differential scanning calorimetry

The thermal stability of P117G was measured as a function of pH by high-sensitivity differential scanning calorimetry. The transitions were reversible under all conditions studied. Figure 1 shows the apparent molar heat capacity of P117G as a function of temperature obtained at pH values of 7.0, 4.1, 3.5, and 3.0 and a salt concentration of 0.1 M. It is clear that the protein is destabilized upon lowering the pH and that the transition becomes absent at pH 3. At pH 7, the T_m (defined as the temperature of the maximum in the heat capacity function) of P117G is 58.5 °C, which is about 5 °C higher than that of the wild-type protein (Shortle et al., 1988). At pH 4.1, the T_m is lowered to 45.4 °C, and at pH 3.5, to 37.0 °C. Several features can be discerned from the experiments shown in Figure 1. First, the heat capacity of the native state increases linearly with temperature within the region in which it is experimentally accessible (10–40 °C). Within this temperature range, it is described by the equation:

$$C_{p,N} = 4{,}760 + 26 \cdot t, \qquad (1)$$

where t is the temperature in degrees C. At 20 °C, $C_{p,N}$ is 5,280 cal·(mol·K)$^{-1}$ (0.31 cal·[g·K]$^{-1}$) and the temperature dependence of $C_{p,N}$ is 26 cal·mol^{-1} K^{-2} (1.55·10^{-3} cal·g^{-1} K^{-2}), which are within the range published earlier for other globular proteins (Privalov & Khechinashvili, 1974; Privalov & Makhatadze, 1990). Second, at pH values of 7.0 and 4.1, the heat capacity of the state existing after thermal denaturation coincides with the heat capacity calculated for the completely unfolded and hydrated molecule (Makhatadze & Privalov, 1990). At lower pH values, the heat capacity of the state existing after thermal denaturation has a lower heat capacity than that of the unfolded molecule, suggesting that not all residues are exposed to the solvent and that the protein retains some residual structure after thermal denaturation at low pH. Third, at pH 3.0, a thermal denaturation transition is not visible in the calorimeter. At this pH, the protein is characterized by a heat capacity intermediate between that of the unfolded and native states. A similar result has been obtained recently by Carra et al. (1994a) for the wild-type enzyme and the V66A mutant. Presumably, under those conditions, the protein exhibits some residual structure at all temperatures within the experimentally accessible range. Fourth, the ΔC_p obtained by subtracting the calculated heat capacity of the unfolded state from that of the native state is a function of temperature and can be well approximated by a second-order polynomial of the form:

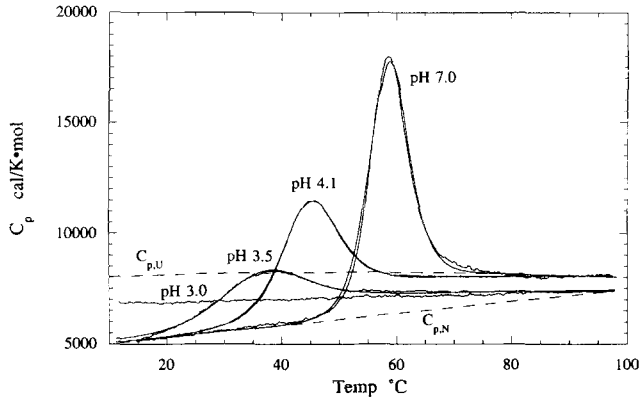

Fig. 1. Partial molar heat capacity versus temperature for P117G as a function of pH at 0.1 M NaCl. Solid lines represent the theoretical curves obtained with the best fitted parameters summarized in Table 1. Dotted lines represent the calculated heat capacities of the unfolded ($C_{p,U}$) and native ($C_{p,N}$) states. At all temperatures at pH 3.0, or at temperatures after the transition at pH 3.5, the protein exists in a partly folded state with a heat capacity about half of that of the unfolded state.

$$\Delta C_p(T) = [2{,}100 + 49.7 \cdot (T - T_R) - 0.11 \cdot (T^2 - T_R^2)] \pm 200, \qquad (2)$$

where the reference temperature T_R has been chosen as 323.15 K (50 °C) and T is given in degrees K. The reported error represents the uncertainty window in the heat capacity determination. According to the above equation, ΔC_p decreases from about 2.1 kcal·(mol·K)$^{-1}$ at 50 °C to less than 1 kcal·(mol·K)$^{-1}$ at 100 °C. A similar second-order temperature dependence has been reported previously for α-lactalbumin (Griko et al., 1994) and barnase (Martinez et al., 1994). For staphylococcal nuclease, the temperature dependence of ΔC_p has not been reported before. Literature values range between 1.9 kcal·(mol·K)$^{-1}$

(Griko et al., 1988), 2.0–2.36 kcal·(mol·K)$^{-1}$ (Calderon et al., 1985), 2.2 kcal·(mol·K)$^{-1}$ (Tanaka et al., 1993), and 2.1 kcal·(mol·K)$^{-1}$ (Carra et al., 1994a, 1994b) for the complete unfolding of the wild-type protein. All of these values are very close to the one obtained in this paper for P117G.

Experiments were performed at different protein concentrations ranging between 0.9 and 5.3 mg/mL (54–315 μM). It has been reported previously that at high concentrations the heat-denatured state of staphylococcal nuclease tends to aggregate, resulting in a concentration dependence of the transition parameters (Tanaka et al., 1993). Within the concentration range examined in this paper, no significant concentration dependence was observed. At pH 4.1, a difference in transition temperature of less than 0.3 °C was observed and, at pH 3.5, a difference of 0.4 °C upon changing the concentration between 0.9 and 5.3 mg/mL. Also, the ratio of the van't Hoff to the calorimetric enthalpy ($\Delta H_{vH}/\Delta H$) never exceeded a value of unity as would have been expected if significant aggregation were present during the transition (see below). This conclusion is similar to that obtained by Carra et al. (1994a), who did not observe significant aggregation within the same concentration range for the wild-type protein. Certainly, at much higher protein concentrations, significant aggregation might be expected as reported by Tanaka et al. (1993).

Analysis of the heat capacity function

The curves in Figure 1 were analyzed as described previously (Freire & Biltonen, 1978; Montgomery et al., 1993) in terms of a general partition function formalism in order to obtain the thermodynamic parameters (ΔH, ΔS, and ΔC_p) for each state that becomes significantly populated during the transition. The main difference is that, in the present analysis, the heat capacities are considered to be temperature-dependent as described in the Materials and methods. The thermodynamic parameters resulting from the nonlinear least-squares analysis of these transitions are summarized in Table 1. The solid lines in the figure represent the theoretical curves obtained with the best fitting parameters summarized in Table 1. At pH values of 7.0 and 4.1, the transition is well accounted for by 2 states. In both cases, the van't Hoff and calorimetric enthalpies are equal within the experimental uncertainties. At 50 °C, the heat capacity change for the transition measured directly from individual scans averages 2.1 ± 0.2 kcal·(mol·K)$^{-1}$. This value is similar in magnitude to the one obtained from the temperature dependence of the enthalpy change in this pH range (2.3 kcal·[mol·K]$^{-1}$).

At pH 3.5 and 0.1 M NaCl, the transition also obeys a 2-state mechanism. However, the heat capacity after thermal denaturation is significantly lower than that obtained at pH 7.0. This is also reflected in the measured ΔC_p value, which is close to 1.0 kcal·(mol·K)$^{-1}$ at 50 °C, about half of the value obtained at pH 7.0, suggesting that under these conditions the protein is not fully unfolded after thermal denaturation, and that it preserves a significant number of hydrophobic residues buried from the solvent water. This partly folded state satisfies the thermodynamic definition of a compact denatured state. At pH 3.0 the transition is no longer visible in the calorimeter. The heat capacity at low temperatures is higher than that of the native state but lower than that of the unfolded state. The heat capacity of this state is similar to that of the thermally denatured state at pH 3.5. Under these conditions the protein exists in the partly folded state at all temperatures between 0 and 100 °C.

The parameters summarized in Table 1 permit calculation of ΔH, ΔS, and ΔC_p at different temperatures. Figure 2 shows the calculated relative enthalpies of the unfolded state and the low-pH, partly folded state as a function of temperature. The curvature visible at high temperatures is due to the temperature dependence of ΔC_p. The most important conclusion from this analysis is that, at temperatures lower than 38 °C, the partly folded state is enthalpically higher than the unfolded state. A similar behavior has been observed before for the molten globule state of apo-α-lactalbumin (Griko et al., 1994) and appears to be a characteristic signature for compact intermediates (Xie & Freire, 1994a, 1994b). It must be noted that a linear least-squares analysis up to 70 °C (as indicated in the figure) yields a ΔC_p value of 2.4 kcal·(mol·K)$^{-1}$ for the unfolded state and 1.3 kcal·(mol·K)$^{-1}$ for the intermediate.

Figure 3 shows the heat capacity function obtained at pH 3.5 and 0.5 M NaCl. At this salt concentration, the transition is characterized by 2 well-defined peaks. This behavior is similar to that observed for some other mutants of staphylococcal nuclease (Carra et al., 1994a). The first peak has similar thermo-

Table 1. *Summary of deconvolution analysis of differential scanning calorimetry results for P117G*[a]

	T_m0 (°C)	$\Delta H(T_m0)$ (cal/mol)	$\Delta C_p(T_m0)$ (cal/mol·K)	b (cal/K^2·mol)	c (cal/K^3·mol)
0.1 M NaCl					
pH 7.0	58.2 ± 0.1	93,000 ± 1,000	2,000 ± 100	49.7 ± 1	−0.107 ± 0.001
pH 4.1	43.6 ± 0.2	59,800 ± 2,000	2,050 ± 135	51.2 ± 0.5	−0.108 ± 0.001
pH 3.5	33.1 ± 0.2	33,000 ± 1,000	1,360 ± 100	21 ± 1	−0.060 ± 0.001
0.5 M NaCl					
pH 3.5					
Transition 1	33.9 ± 0.3	38,500 ± 2,000	1,050 ± 1,000	26.7 ± 2	−0.061 ± 0.001
Transition 2	60.4 ± 0.4	21,500 ± 2,500	510 ± 50	36 ± 2	−0.060 ± 0.002

[a] T_m0 is the temperature at which $\Delta G = 0$. $\Delta H(T_m0)$ and $\Delta C_p(T_m0)$ are the values of ΔH and ΔC_p at T_m0. At any temperature $\Delta C_p(T) = \Delta C_p(T_m0) + b_i \cdot (T - T_m0) + c_i \cdot (T^2 - T_m0^2)$, where the temperature is in degrees K. The errors in the table correspond to errors in the deconvolution parameters from nonlinear least-squares analysis (Montgomery et al., 1993). Absolute errors in temperature determination are ±0.3 °C, errors in enthalpy determination are ±5%, and errors in heat capacity ±10%.

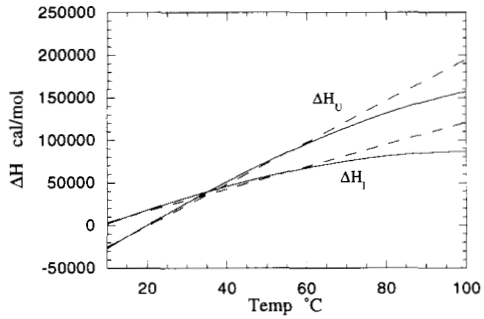

Fig. 2. The calculated relative enthalpy of the unfolded state (ΔH_U) and the low pH partly folded state (ΔH_I) as a function of temperature. The solid lines were calculated with the thermodynamic parameters in Table 1 and include a temperature dependent ΔC_p. The dotted lines represent the results of a linear least-squares fitting up to 70 °C. At temperatures below 38 °C, the enthalpy of the partly folded state is higher than that of the unfolded state. Stabilization of the intermediate at low temperatures must be entropic because it is enthalpically less favorable than the unfolded state.

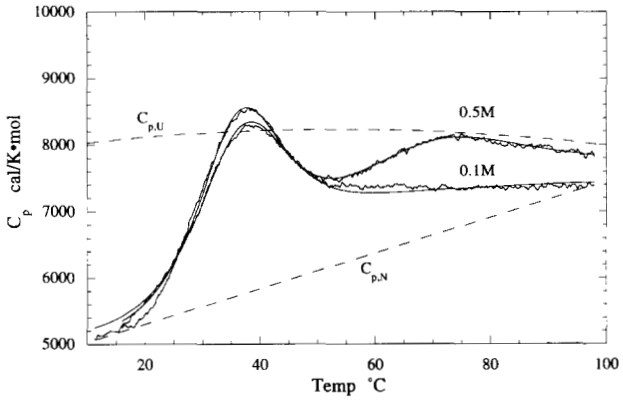

Fig. 3. Partial molar heat capacity of P117G at pH 3.5 versus temperature and 2 different NaCl concentrations. The buffer used was 10 mM glycine-HCl, 1 mM EDTA. Solid lines represent the theoretical curves obtained with the best fitted parameters summarized in Table 1. At 0.5 M NaCl, the heat capacity function exhibits 2 clearly distinguishable peaks and can be well accounted for by 3 states. The first peak corresponds to the transition between the native state and a partly folded state and is not affected by the change of ionic strength. The second peak corresponds to the transition between the partly folded state and the unfolded state. Dotted lines represent the calculated heat capacities of the unfolded ($C_{p,U}$) and native ($C_{p,N}$) states.

dynamic parameters to those observed at 0.1 M NaCl and its T_m is quite insensitive to the change in ionic strength. The ΔC_p for the total transition (first and second peaks) is close to that obtained for the complete unfolding of the protein at higher pH values, suggesting that, after the second peak, the polypeptide is essentially unfolded. Close inspection of the data in Figure 3 suggests that the heat capacity after the second peak might be slightly lower than that of the unfolded state; however, the difference is small and might be due to experimental uncertainties. The heat capacity for the first transition estimated from the deconvolution of the heat capacity function is 0.85 kcal·(mol·K)$^{-1}$ at 50 °C, which is close to the value measured for the transition at 0.1 M NaCl. Also, the enthalpy changes for the 2 transitions are similar (33 and 38 kcal·mol^{-1}, respectively).

From a thermodynamic point of view, it can be concluded that the first peak observed at pH 3.5 and 0.5 M NaCl corresponds to the transition from the native state to the compact denatured state, and the second one to the transition from the compact denatured state to the unfolded state. As shown in the figure, only 3 states are necessary to quantitatively account for the data, indicating that both the transition from the native state to the intermediate and the subsequent transition from the intermediate to the unfolded state are fully cooperative. This result should be contrasted with the one obtained previously for α-lactalbumin (Griko et al., 1994). In this case, the first peak corresponding to the transition from the native to the molten globule is fully cooperative, whereas the transition from the molten globule to the unfolded state occurs in a rather noncooperative fashion. For P117G, the $\Delta H_{vH}/\Delta H$ ratio is close to 1, whereas for α-lactalbumin it is in the range of 0.3–0.5 (Griko et al., 1994). At high temperature, the addition of salt stabilizes the unfolded state of P117G, whereas the compact denatured state is stable at low ionic strengths. The solid lines in Figure 3 represent the theoretical curves obtained by the best fitting parameters summarized in Table 1.

CD spectroscopy

In order to characterize the structural changes associated with the transitions, CD measurements of P117G were performed at different pH values and temperatures. Figure 4 shows the far-UV CD spectra at pH values of 4.1 and 3, and 2 temperatures. At 25 and 72 °C, respectively, the spectra obtained at pH 4.1 corresponds to the native state and the unfolded state according to the calorimetry experiments. They are consistent with the results reported by other authors (Shortle & Meeker, 1989; Shortle & Abergunawardana, 1993; Carra et al., 1994a). At pH 3.0, the spectra are similar at low and high temperatures, consistent with

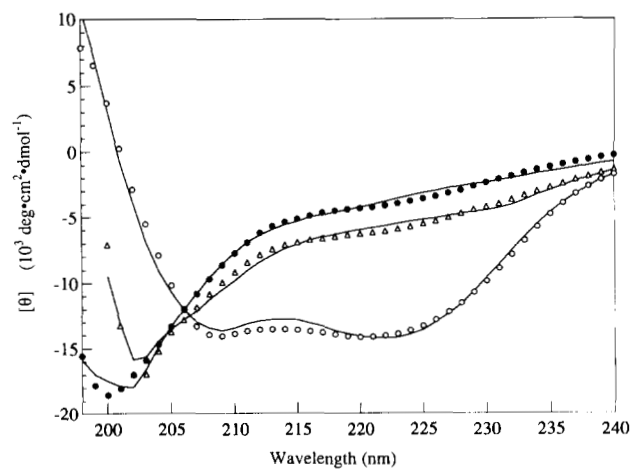

Fig. 4. Far UV CD spectra of P117G at pH values of 4.1 and 3.0, 0.1 M NaCl and different temperatures. The buffers were the same as those in the differential scanning calorimetry experiments. Open circles represent the spectrum at pH 4.1 and 25 °C (native state); open triangles represent the spectrum at pH 4.1 and 72 °C (unfolded state); filled circles correspond to the spectra at pH 3.0 (partly folded state) measured at 25 °C. Solid lines represent the theoretical curves obtained with the program CCAFAST, which implements the convex constraint algorithm (Perczel et al., 1992).

the absence of a transition. At this pH, the spectra show no evidence of α-helical structure.

A quantitative estimation of the secondary structural content in the intermediate state was performed by deconvoluting the CD spectra using the convex constraint algorithm developed by Perczel et al. (1992). Figure 4 also shows the experimental spectra and the theoretical curves calculated with the best fitting parameters. The secondary structural content estimated for the native state (pH 4.1 and 25 °C) is 32% α-helix, 24% β-sheet, and 43% coil, respectively. These values are consistent with the X-ray crystallographic structure, which indicates that 26% of the residues are in α-helix and 23% in β-sheet conformations. At pH 4.1 and 72 °C, the spectrum represents the unfolded state according to the calorimetric data and the fitting indicates that 99% of the structure is indeed in an unordered coil conformation. At pH 3.0 and 25 °C, the protein exists in the compact denatured state according to the calorimetric experiments. Deconvolution of the CD spectrum recorded under these conditions yielded 3% α-helix, 21% β-sheet, and 76% unordered coil structure. This result suggests that the compact denatured state maintains a significant amount of the β-sheet structure and that most of the α-helix structure is absent.

Structural thermodynamic analysis

Previously, several laboratories have shown that the heat capacity change associated with the unfolding of the native state of a protein can be expressed as a linear combination of the differences in polar (ΔASA_{pol}) and apolar (ΔASA_{ap}) solvent-accessible surface areas between those states (Murphy et al., 1992; Murphy & Freire, 1992; Spolar et al., 1992):

$$\Delta C_p = 0.44 \cdot \Delta ASA_{ap} - 0.26 \cdot \Delta ASA_{pol}, \quad (3)$$

where 0.44 and −0.26 are the elementary contributions per Å^2 of apolar and polar area exposed to water in cal·(K·mol)$^{-1}$. The empirical parameterization was performed on the existing database, which is composed of temperature-independent ΔC_p values obtained mainly from the temperature dependence of ΔH or individual ΔC_p values obtained mainly within the 30–70 °C range (Murphy et al., 1992). These values are expected to correspond to those obtained from the dotted lines in Figure 2. All our accessible surface area calculations of protein structures and partly folded states were analyzed as described previously (Murphy et al., 1992) using the implementation of Lee and Richard's algorithm (Lee & Richards, 1971) in the program ACCESS (S.R. Presnell, University of California, San Francisco), with a probe radius of 1.4 Å and a slice width of 0.25 Å.

The bulk of the enthalpy change can also be expressed as a linear combination of the changes in polar and apolar solvent-accessible surface areas:

$$\Delta H(T) = \mathrm{a}(T) \cdot \Delta ASA_{ap} + \mathrm{b}(T) \cdot \Delta ASA_{pol} \quad (4)$$

$$\Delta H(T) = \mathrm{a}(T_R) \cdot \Delta ASA_{ap} + \mathrm{b}(T_R) \cdot \Delta ASA_{pol} + \Delta C_p \cdot (T - T_R), \quad (4a)$$

where T_R is an appropriately chosen reference temperature. At 60 °C, which corresponds to the median transition temperature for the proteins in the database, the enthalpy change can be written as (Xie & Freire, 1994a):

$$\Delta H(60) = 31.4 \cdot \Delta ASA_{pol} - 8.44 \cdot \Delta ASA_{ap}. \quad (5)$$

The choice of 60 °C as the reference temperature minimizes extrapolation errors due to uncertainties and nonlinearity effects on ΔC_p. At 60 °C, the average error between the experimental and calculated values is 6%. Under most conditions, Equations 4 and 5 account for more than 90% of the enthalpy change of unfolding. The additional terms correspond mainly to the enthalpies associated with protonation or the effects of specific ligands, if present. Those additional contributions need to be taken into account explicitly, especially at low temperatures in which the contribution given by Equation 5 is close to zero. The protonation of carboxylic groups has an enthalpy close to −1 kcal·mol^{-1} and that of histidyl groups is close to −7 kcal·mol^{-1}.

For P117G, the complete unfolding of the native structure is accompanied by an increase in ΔASA_{ap} of 8,120 Å^2 and an increase in ΔASA_{pol} of 5,050 Å^2, which correspond to a predicted ΔC_p of 2.3 kcal·(mol·K)$^{-1}$ and a ΔH of 87 kcal·mol^{-1} at the transition temperature of 58.2 °C obtained at pH 7.0. These values are very close to the experimental values summarized in Table 1.

By rearranging Equations 3–5, it is possible to estimate that the transition from the native state to the partly folded state is accompanied by a ΔASA_{ap} of 4,322 Å^2 and a ΔASA_{pol} of 3,249 Å^2. This result indicates that a larger proportion of polar than apolar residues is exposed to the solvent in the partly folded state. In fact, about 50% of the hydrophobic core is preserved in the partly folded state, whereas only 36% of the polar area remains buried from the solvent in the intermediate. This pattern of behavior is characteristic of compact intermediates.

Combinatorial generation of partly folded states

Previously, we have presented an algorithm aimed at generating native-like partly folded states using the crystallographic or NMR solution structure of a protein as a template (Xie & Freire, 1994a, 1994b). This algorithm considers the protein as being formed by an arbitrary number of folding units. Each folding unit can be either in the native or unfolded states. For a total of N different folding units a total of 2^N states are generated with the computer by folding and unfolding the folding units in all possible combinations. The number of folding units determines the resolution of the analysis. Usually, secondary structure elements are considered as the starting point for partitioning. The resolution of the partitioning grid is then increased by further subdividing the protein into smaller units comprising only parts of secondary structure elements. This process can be repeated to the desired level of resolution.

Once the ensemble of states is generated, the energetics of each state is calculated using the structural parameterization discussed above (see Xie & Freire, 1994a, 1994b, for details). The resulting energetics is used to identify those partly folded states that are expected to have the highest probability of being populated. Specific thermodynamic parameters (e.g., ΔH and ΔC_p) can be compared to the experimental values. This procedure has been

Table 2. *Scheme showing the partitioning of P117G into 7 folding units corresponding to elements of secondary structure*

Folding units	Residues	Secondary structure
1	6–37	3β
2	38–51	Loop
3	52–70	α1
4	71–98	3β
5	99–109	α2
6	110–120	Loop
7	121–141	α3, loop

shown to correctly predict the structural determinants of the folding intermediates of a number of proteins (Xie & Freire, 1994a, 1994b).

The analysis of P117G was initiated by partitioning the protein into 7 folding units corresponding to the elements of secondary structure shown in Table 2.

In the structure of P117G, the first 5 residues are disordered. The first unit includes 3 β-strands: β1 (residues 10–19), β2 (residues 22–27), and β3 (residues 30–36). The second unit corresponds to a loop (residues 38–51) and the third unit is defined by the first α-helix (residues 54–68). Three β-strands, β4 (residues 71–76), β5 (residues 88–95), and β6 (residues 97–98), form the fourth unit. The fifth unit corresponds to the second α-helix (residues 99–106). The sixth unit is an 11-residue loop (residues 110–120) and the last unit includes the third α-helix (residues 135–141).

The internal consistency of the partitioning scheme (Table 2) was checked by shifting the boundaries of each folding unit upward and downward in sequence by 1 and 2 amino acid residues. The results were very similar in all cases. In addition, the resolution of the initial partitioning was increased by dividing the folding units into smaller units as follows:

{6, 27} {28, 37} {38, 51} {52, 70} {71, 82} {83, 98} {99, 109} {110, 120} {121, 141} (Scheme A)

{6, 27} {28, 37} {38, 51} {52, 60} {61, 70} {71, 82} {83, 98} {99, 109} {110, 120} {121, 141} (Scheme B)

{6, 19} {20, 27} {28, 37} {38, 51} {52, 60} {61, 70} {71, 82} {83, 95} {96, 98} {99, 109} {110, 120} {121, 141}, (Scheme C)

where each bracketed pair represents 1 folding unit. Scheme A is composed of 9 folding units in which the 2 units were created by considering β3 and β4 as 2 separate units. In scheme B, 1 additional unit was created by breaking the long helix (residues 54–68) into 2 separate units. In scheme C, each β-strand was considered as a separate folding unit resulting in 12 folding units and a total of 4,096 states. The results obtained with all these schemes were similar; therefore, for simplicity, the discussion will be centered around the scheme in Table 2.

Equations 3–5 were used to estimate the energetics of all the states of P117G generated by the above combinatorial approach. The probability of each state was calculated according to the standard equation:

$$P_i = e^{-\Delta G_i/RT} / \Sigma e^{-\Delta G_i/RT}, \quad (6)$$

where ΔG_i is the Gibbs free energy of state i, R the gas constant, and T the absolute temperature. The sum in the denominator runs over all the states and defines the partition function.

Because compact intermediates preserve a sizable hydrophobic core, they are characterized by: (1) a lower heat capacity than the unfolded state and (2) a higher enthalpy than the unfolded state at low temperatures (Griko et al., 1994). These 2 properties are also identified in the search algorithm.

Figure 5A, B, and C shows the thermodynamic parameters for each of the 128 states generated by the computer for the scheme shown in Table 2. Figure 5A shows the relative enthalpy of each state at 25 °C. It is clear that at this temperature the unfolded state is not the highest enthalpy state. Some partly folded states, particularly states 79, 60, and 45 have a higher enthalpy than the unfolded state. These states are also characterized by having a heat capacity lower than the average value corresponding to their degree of unfolding (Fig. 5B). The reason for this behavior is that these states bury an anomalously large hydrophobic surface from the solvent. A consequence of this structural property is that these states have a more favorable solvent-related entropy than those states that expose to the solvent a higher proportion of hydrophobic surface. The net result is that these states end up with a more favorable intrinsic free energy and a higher probability of being populated, as shown in Figure 5C. It is clear from the figure that, at 25 °C, the native state is the state with the lowest free energy and therefore the most highly populated. At 65 °C, state 79 and other partly folded states (e.g., states 60, 45, 30) have lower free energies than both the folded and unfolded states and are therefore the most highly populated states. As the temperature increases, the unfolded state progressively becomes the most highly populated state. The thermodynamic parameters for the states with the highest probability of being populated are summarized in Table 3.

It is clear from Table 3 that folding unit 1 is folded in all partly folded states predicted to have a high probability. This folding unit corresponds to the first 3 strands (β1, β2, β3) of the β subdomain (residues 6–37). Folding unit 4, on the other hand, is predicted to be folded in 5 of the 7 partly folded states in Table 3. Folding unit 4 corresponds to the remaining 3 β-strands (β4, β5, β6) of the β subdomain (residues 71–98). These calculations predict that the β subdomain is the most stable structure of the molecule and that the partly folded intermediate is characterized by having the β subdomain intact or almost intact. On the other hand, folding units 3, 5, and 7, which correspond to the 3 α-helices, are unfolded in most of the states in Table 3. These predictions agree with the CD experiments showing the loss of α-helical structure in the low pH intermediate.

Among the states in Table 3, state 79 is especially noteworthy because it has the highest probability and contains the consensus structure. Also, the energetics of this state is similar to that determined experimentally for the low pH intermediate. The heat capacity of state 79 is 1.3 kcal·(mol·K)$^{-1}$, compared with 1.4 kcal·(mol·K)$^{-1}$ for the partly folded state at pH 3.5. At 34 °C, the relative enthalpy of state 79 is 28 kcal·mol^{-1} compared with the experimental value of 33–39 kcal·mol^{-1} mea-

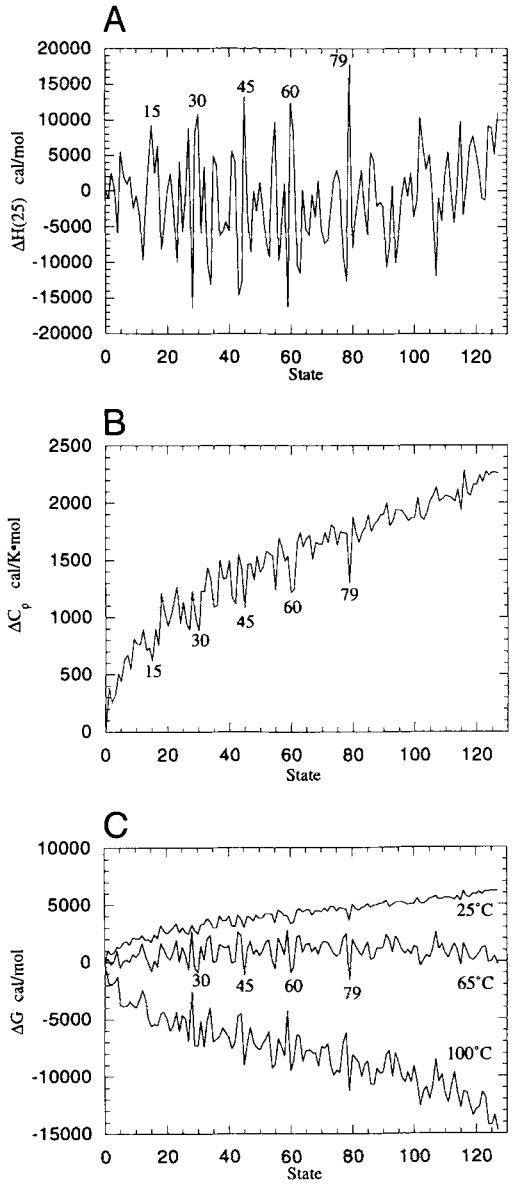

Fig. 5. Relative enthalpy at 25 °C, $\Delta H(25)$ **(A)**; heat capacity, ΔC_p **(B)**; and coarse free energy at 25 °C, 65 °C, and 100 °C **(C)** for the 128 simulated states of P117G. The protein states have been numbered according to their degree of unfolding; the native state being state 0 and the unfolded state being state 127. The states that exhibit the highest intrinsic probabilities are indicated in the figure. At low and high temperatures, the native and the unfolded states exhibit the lowest free energies, respectively. Within the transition region or immediately after, some partly folded states have a lower intrinsic free energy than either the native or unfolded states. These states have the highest probability of being stabilized by pH, ionic strength, or other factors and become highly populated equilibrium folding intermediates.

sured at pH 3.5. Although the predicted and experimental ΔC_p values are very close, the predicted ΔH value appears to be somewhat smaller than the experimental value. A possible reason for this difference is that the atomic packing and consequently the van der Waals interactions are not as tight in the partly folded state as in the native state. In our calculations it is assumed that the folded regions remain as in the native state.

Table 3. *Thermodynamic parameters of most probable partly folded intermediates*

State	Binary code[a]	ΔC_p kcal·(mol·K)$^{-1}$	$\Delta H(25)$ kcal·mol^{-1}
15	0000011	0.65	8.4
30	0100011	0.91	9.7
45	0100111	1.1	11.8
60	0110101	1.3	10.8
79	0110111	1.3	16.1
102	0111101	1.9	7.9
115	0111111	2.0	7.3
127	1111111	2.3	8.1

[a] In this binary code, cooperative folding units in the unfolded state are represented by a 1 and cooperative folding units in the folded state are represented by a 0, e.g., the first 0 on the left indicates that the first cooperative unit is folded.

If this is the case, the difference of ≈8 kcal·mol^{-1} between the experimental and predicted values might represent the enthalpy associated with the loosening of the native packing. This loosening, however, is not as severe as to allow water penetration judging by the agreement between the ΔC_p values. It is known that ΔC_p of hydration is to a large extent insensitive to the packing density (Privalov & Gill, 1988; Murphy & Gill, 1991).

Figure 6 illustrates the basic structural features of state 79 (0110111). As mentioned before, in this state the β subdomain is folded, whereas the rest of the molecule is unfolded. Roughly 40% of the amino acid residues are in a folded conformation, but close to 60% of the hydrophobic core is already buried from the solvent. The extremely high proportion of hydrophobic surface burial provides the main stabilizing force for the folding intermediate. It should be remembered that, at temperatures below 38 °C, this state is enthalpically unfavorable relative to the unfolded state (Fig. 2), and therefore its stabilization must be of an entropic origin. The required entropy arises mostly from the solvent-related entropy associated with the hydrophobic effect.

Conclusions

In this work, the energetics of a compact denatured state of P117G was studied by high-sensitivity differential scanning calorimetry. In agreement with previous results obtained with the wild-type and other mutants of staphylococcus nuclease (Carra et al., 1994a, 1994b, 1994c), P117G undergoes a 2-state thermal denaturation transition at neutral pH. Under these conditions, the thermally denatured protein is in a fully hydrated unfolded state judging by the absolute heat capacity value after the transition. At pH 3.5, the protein undergoes a cooperative thermal denaturation transition to a compact denatured state. The heat capacity of this state is approximately half that of the unfolded state. The CD experiments indicate that the α-helical regions are greatly disrupted or not present in the compact denatured state. At pH 3.0, there is no transition observed in the heat capacity function. The protein remains in the compact denatured state at all temperatures between 10 and 100 °C. Upon increasing the

Fig. 6. Ribbon diagram of state 79 (0110111) of staphylococcal nuclease P117G variant. The dark regions represent the folded parts of the molecule in the partly folded state (residues 6–37 and 71–98), which correspond to the β subdomain. White regions represent the parts of the protein that are disordered (residues 38–70 and 99–141). The figure was generated with the program MOLSCRIPT (Kraulis, 1991).

ionic strength, for example at pH 3.5 and 0.5 M NaCl, the protein undergoes a second transition that corresponds to the complete unfolding of the compact denatured state.

The structure of the partly folded intermediate of P117G was modeled by structural thermodynamic analysis of a large ensemble of native-like partly folded states. The results of this analysis indicate that the most probable structure of the intermediate is one in which the β subdomain is intact or almost intact, whereas the other parts of the molecule are unfolded. This conclusion is supported by the CD experiments. More interestingly, this structure is also very close to that of a kinetic folding intermediate of P117G revealed by NMR hydrogen exchange experiment (Jacobs & Fox, 1994). This suggests that the stable compact denatured state is the kinetic intermediate being further stabilized. The same phenomena have also been observed for other proteins (Ikeguchi et al., 1986; Jennings & Wright, 1993; Kippen et al., 1994).

The predicted heat capacities for the unfolded and compact denatured states are consistent with the experimental results. However, the predicted enthalpy of the compact denatured state is 8 kcal·mol^{-1} or about 25% less than the experimentally measured value. This difference could be due to the oversimplification of assuming native-like packing interactions for the folded regions in the intermediate (i.e., that the structural parameterization of the enthalpy obtained for the native state also applies to the partly folded intermediate). According to the NMR results of Shortle and Abergunawardana (1993) for the 136-residue nonsense fragment of staphylococcal nuclease, many resonances are missing in the compact denatured state, suggesting significant rotameric disorder. The differences between such state and a state that preserves the native packing interactions will be thermodynamically reflected on a larger conformational entropy and a larger enthalpy. The larger conformational entropy would originate from the increased disorder and the larger enthalpy from the decrease in van der Waals interactions. These two quantities will at least partially compensate each other, making a smaller overall contribution to the Gibbs free energy.

Under certain conditions (e.g., 0.5 M NaCl, pH 3.5), the partly folded state undergoes a highly cooperative transition to the unfolded state. This observation agrees with previous results obtained with the large fragment of staphylococcal nuclease that contains mainly the β-sheet structure (Gittis et al., 1993). In fact, thermal denaturation experiments on the isolated fragment indicate that, at pH 3.9, the fragment unfolds at 76 °C, with an enthalpy of 30 kcal·mol^{-1} (Griko, pers. comm.). This enthalpy is similar to that expected for the second transition obtained at 0.5 M NaCl when extrapolated at 76 °C using the parameters in Table 1. The fact that a molecule largely devoid of the tight packing interactions existing in the native state is able to undergo cooperative folding/unfolding suggests that tight packing might not be the only determinant of cooperativity. In fact, during the last few years, some "molten globules" have been shown to undergo temperature-induced cooperative transitions (cytochrome *c* [Hagihara et al., 1994]), others diffuse transitions (α-lactalbumin [Griko et al., 1994]), and some others no transitions at all (apomyoglobin [Griko & Privalov, 1994]). It appears that the absence of temperature-induced cooperative folding/unfolding transitions cannot be considered as a general property of these equilibrium intermediates.

Materials and methods

Protein

The protein was prepared and purified as previously described (Jacobs & Fox, 1994). The protein was dialyzed against 4 L of 10 mM phosphate buffer, 1 mM EDTA for the experiments at pH 7.0; against 10 mM acetate, 1 mM EDTA for pH 4.1; and 10 mM glycine-HCl, 1 mM EDTA for pH 3.5 and pH 3.0. NaCl concentration was 0.1 M in all experiments unless otherwise indicated. Protein concentration was determined from the absorbance at 280 nm, with an extinction coefficient of 0.93 for a 1 mg·mL^{-1} solution (Fuchs et al., 1967). The protein sample was degassed for 10–15 min before experiment.

Differential scanning calorimetry

The calorimetric studies were performed with a DASM-92 differential scanning calorimeter developed at the Biocalorimetry Center using a protein concentration of 0.9–5.3 mg·mL^{-1}. The calorimetric unit was interfaced to a computer using an A/D converter board for automatic data collection. All experiments were performed at a scanning rate of 60 °C per h. Reversibility was assessed by scanning the same sample twice. The apparent heat capacity of the protein was obtained as described by Privalov and Potekhin (1986). Data reduction and analysis were performed with software developed in this laboratory.

Analysis of the heat capacity function

Deconvolution of the excess heat capacity function ($\langle\Delta C_p\rangle$) was performed as described previously (Freire & Biltonen, 1978; Montgomery et al., 1993) except that the relative heat capacity of each state was approximated by a second-order polynomial of the form:

$$\Delta C_{p,i}(T) = a_i + b_i \cdot T + c_i \cdot T^2. \quad (7)$$

Accordingly, the relative enthalpies and entropies become:

$$\Delta H_i(T) = \Delta H_i(T_R) + a_i \cdot (T - T_R) + (b_i/2) \cdot (T^2 - T_R^2) + (c_i/3) \cdot (T^3 - T_R^3) \quad (8)$$

$$\Delta S_i(T) = \Delta S_i(T_R) + a_i \cdot \ln(T/T_R) + b_i \cdot (T - T_R) + (c_i/2) \cdot (T^2 - T_R^2), \quad (9)$$

where T_R is a reference temperature usually taken as $T_m 0$, the temperature at which the Gibbs free energy is zero. For convenience, Equation 1 can be written as:

$$\Delta C_{p,i}(T) = \Delta C_{p,i}(T_R) + b_i \cdot (T - T_R) + c_i \cdot (T^2 - T_R^2), \quad (10)$$

where the first term on the right is the heat capacity change at the reference temperature. In Equations 7–10, the temperature is given in degrees K.

Circular dichroism

CD spectra were obtained from 240 to 190 nm with a JASCO J-710 Spectropolarimeter. The sample was scanned 5 times using a protein concentration of 0.3 $mg \cdot mL^{-1}$ and a 1-mm rectangular cell. The buffers used were identical to those used in the calorimetric experiments. Temperature was maintained by using a Haake F3 programmable circulating water bath connected to a water-jacketed cell holder. Temperature was monitored using a Microtherm 1006 thermometer and a S/N117.C temperature probe. Mean residue ellipticities were obtained using the standard equation after subtracting the buffer scan:

$$[\theta] = \theta_{obs}/(10 \cdot C_r \cdot l),$$

where C_r is the mean residue molar concentration and l is the pathlength of the cell in centimeters. Estimation of secondary structure composition was made by deconvolution of the CD data with the program CCAFAST, which implements the convex constraint algorithm (Perczel et al., 1992). Thirty iterations were performed for each fitting. Due to the scattering at low wavelengths, only the part of the spectrum from 198 to 240 nm was included in the fitting as shown in the figure.

Acknowledgments

This work was supported by grants from the National Institutes of Health (RR-04328, GM-37911, and NS-24520) and the National Science Foundation (MCB-9118687) (E.F.); and the Howard Hughes Medical Institute and the National Institutes of Health (AI23923) (R.O.F). We thank Marc Jacobs for preparing the nuclease P117G protein. We also thank John Carra and Peter Privalov for many discussions and for sharing their data prior to publication.

References

Calderon RO, Stolowich NJ, Gerlt JA, Sturtevant JM. 1985. Thermal denaturation of staphylococcal nuclease. *Biochemistry 24*:6044–6049.

Carra JH, Anderson EA, Privalov PL. 1994a. Thermodynamics of staphylococcal nuclease denaturation I. The acid-denatured state. *Protein Sci 3*:944–951.

Carra JH, Anderson EA, Privalov PL. 1994b. Thermodynamics of staphylococcal nuclease denaturation II. The A state. *Protein Sci 3*:952–959.

Carra JH, Anderson EA, Privalov PL. 1994c. Three-state thermodynamic analysis of the denaturation of staphylococcal nuclease mutants. *Biochemistry 33*:10842–10850.

Evans PA, Dobson CM, Kautz RA, Hatfull G, Fox RO. 1987. Proline isomerism in staphylococcal nuclease characterized by NMR and site-directed mutagenesis. *Nature 329*:266–268.

Freire E, Biltonen RL. 1978. Statistical mechanical deconvolution of thermal transitions in macromolecules. I. Theory and application to homogeneous systems. *Biopolymers 17*:463–479.

Freire E, Xie D. 1994. Thermodynamic prediction of structural determinants of the molten globule state of proteins. *Biophys Chem 51*:243–251.

Fuchs S, Cuatrecasas P, Anfinsen CB. 1967. An improved method for the purification of staphylococcal nuclease. *J Biol Chem 242*:4768–4770.

Gittis AG, Stites WE, Lattman EE. 1993. The phase transition between a compact denatured state and a random coil state in staphylococcal nuclease is first-order. *J Mol Biol 232*:718–724.

Goto Y, Nishikiori S. 1991. Role of electrostatic repulsion in the acidic molten globule of cytochrome *c*. *J Mol Biol 222*:679–686.

Griko Y, Freire E, Privalov PL. 1994. Energetics of the alpha-lactalbumin states. A calorimetric and statistical thermodynamic study. *Biochemistry 33*:1889–1899.

Griko YV, Privalov PL. 1994. Thermodynamic puzzle of apomyoglobin unfolding. *J Mol Biol 235*:1318–1325.

Griko YV, Privalov PL, Sturtevant JM, Venyaminov SY. 1988. Cold denaturation of staphylococcal nuclease. *Proc Natl Acad Sci USA 85*:3343–3347.

Hagihara Y, Tan Y, Goto Y. 1994. Comparison of the conformational stability of the molten globule and native states of cytochrome *c*: Effects of acetylation, urea and guanidine-hydrochloride. *J Mol Biol 237*:336–348.

Hughson FM, Wright PE, Baldwin RL. 1990. Structural characterization of a partly folded apomyoglobin intermediate. *Science 249*:1544–1548.

Hynes TR, Hodel A, Fox RO. 1994. Engineering alternative β-turn types in staphylococcal nuclease. *Biochemistry 33*:5021–5030.

Ikeguchi M, Kuwajima K, Sugai S. 1986. Ca^{2+}-induced alteration in the unfolding behavior of α-lactalbumin. *J Biochem (Tokyo) 99*:1191–1201.

Jacobs MD, Fox RO. 1994. Staphylococcal nuclease folding intermediate characterized by hydrogen exchange and NMR spectroscopy. *Proc Natl Acad Sci USA 91*:449–453.

Jeng MF, Englander SW. 1991. Stable submolecular folding units in a non-compact form of cytochrome *c*. *J Mol Biol 221*:1045–1061.

Jeng MF, Englander SW, Elöve GA, Wand AJ, Roder H. 1990. Structural description of acid-denatured cytochrome *c* by hydrogen exchange and 2D NMR. *Biochemistry 29*:10433–10437.

Jennings PA, Wright PE. 1993. Formation of a molten globule intermediate early in the kinetic folding pathway of apomyoglobin. *Science 262*:892–896.

Kippen AD, Sancho J, Fersht AR. 1994. Folding of barnase in parts. *Biochemistry 33*:3778–3786.

Kraulis PJ. 1991. MOLSCRIPT: A program to produce both detailed and schematic plots of protein structures. *J Appl Crystallogr 24*:946–950.

Kuroda Y, Kidokoro SI, Wada A. 1992. Thermodynamic characterization of cytochrome *c* at low pH. Observation of the molten globule state and of the cold denaturation process. *J Mol Biol 223*:1139–1153.

Kuwajima K. 1989. The molten globule state as a clue for understanding the folding and cooperativity of globular-protein structure. *Proteins Struct Funct Genet 6*:87–103.

Kuwajima K, Okayama N, Yamamoto K, Ishihara T, Sugai S. 1991. The Pro^{117} to glycine mutation of staphylococcal nuclease simplifies the unfolding-folding kinetics. *FEBS Lett 290*:135–138.

Lee B, Richards FM. 1971. The interpretation of protein structures: Estimation of static accessibility. *J Mol Biol 55*:379–400.

Makhatadze GI, Privalov PL. 1990. Heat capacity of proteins. I. Partial molar heat capacity of individual amino acid residues in aqueous solution: Hydration effect. *J Mol Biol 213*:375–384.

Martinez JC, Harrous ME, Filimonov VV, Mateo PL, Fersht AR. 1994. A

calorimetric study of the thermal stability of barnase and its interaction with 3'GMP. *Biochemistry 33*:3919–3926.
Montgomery D, Jordan R, McMacken R, Freire E. 1993. Thermodynamic and structural analysis of the folding/unfolding transitions of DNAK. *J Mol Biol 232*:680–692.
Murphy KP, Bhakuni V, Xie D, Freire E. 1992. The molecular basis of cooperativity in protein folding III: Identification of cooperative folding units and folding intermediates. *J Mol Biol 227*:293–306.
Murphy KP, Freire E. 1992. Thermodynamics of structural stability and cooperative folding behavior in proteins. *Adv Protein Chem 43*:313–361.
Murphy KP, Gill SJ. 1991. Solid model compounds and the thermodynamics of protein unfolding. *J Mol Biol 222*:699–709.
Nakano T, Antonino LC, Fox R, Fink AL. 1993. Effect of proline mutation on the stability and kinetics of folding of staphylococcal nuclease. *Biochemistry 32*:2354–2541.
Perczel A, Park K, Fasman GD. 1992. Analysis of the circular dichroism spectrum of proteins using the convex constraint algorithm: A practical guide. *Anal Biochem 203*:83–93.
Privalov PL, Gill SJ. 1988. Stability of protein structure and hydrophobic interaction. *Adv Protein Chem 39*:191–234.
Privalov PL, Khechinashvili NN. 1974. A thermodynamic approach to the problem of stabilization of globular protein structure: A calorimetric study. *J Mol Biol 86*:665–684.
Privalov PL, Makhatadze GI. 1990. Heat capacity of proteins. II. Partial molar heat capacity of the unfolded polypeptide chain of proteins: Protein unfolding effects. *J Mol Biol 213*:385–391.
Privalov PL, Potekhin SA. 1986. Scanning microcalorimetry in studying temperature-induced changes in proteins. *Methods Enzymol 131*:4–51.
Shortle D, Abergunawardana C. 1993. NMR analysis of the residual structure in the denatured state of an unusual mutant of staphylococcal nuclease. *Curr Biol 1*:121–134.
Shortle D, Meeker AK. 1989. Residual structure in large fragments of staphylococcal nuclease: Effects of amino acid substitutions. *Biochemistry 28*:936–944.
Shortle D, Meeker AK, Freire E. 1988. Stability mutants of staphylococcal nuclease: Large compensating enthalpy–entropy changes for the reversible denaturation reaction. *Biochemistry 27*:4761–4768.
Spolar RS, Livingstone JR, Record MT Jr. 1992. Use of liquid hydrocarbon and amide transfer data to estimate contributions to thermodynamic functions of protein folding from the removal of nonpolar and polar surface from water. *Biochemistry 31*:3947–3955.
Tanaka A, Flanagan J, Sturtevant JM. 1993. Thermal unfolding of staphylococcal nuclease and several mutants forms thereof studied by differential scanning calorimetry. *Protein Sci 2*:567–576.
Xie D, Bhakuni V, Freire E. 1991. Calorimetric determination of the energetics of the molten globule intermediate in protein folding: Apo-α-lactalbumin. *Biochemistry 30*:10673–10678.
Xie D, Freire E. 1994a. Molecular basis of cooperativity in protein folding. V. Thermodynamic and structural conditions for the stabilization of compact denatured states. *Proteins Struct Funct Genet 19*:291–301.
Xie D, Freire E. 1994b. Structure based prediction of protein folding intermediates. *J Mol Biol 242*:62–80.